SEMARAK ILMU PUBLISHING

CFD Letters

Journal homepage:
https://semarakilmu.com.my/journals/index.php/CFD_Letters/index
ISSN: 2180-1363

Performance Evaluation of Different Texture Material Masks to Reduce Airborne Infection

Fatma A-M. Kassem[1,*], Ahmed Farouk AbdelGawad[2], Mofreh M. Nassief[2], A. E. Abu El-Ezz[3], S.H. Samaha[4], Mohamed Adel[2]

[1] Department of Volume and Fluid Flow Metrology, National Institute of Standards (NIS), Giza, Egypt
[2] Department of Mechanical Power Engineering, Faculty of Engineering, Zagazig University, Egypt
[3] Department of Force and Material Metrology, National Institute of Standards (NIS), Giza, Egypt
[4] Materials Testing and Surface Chemical Analysis Metrology, National Institute of Standards (NIS), Egypt

ARTICLE INFO

Article history:
Received 18 December 2022
Received in revised form 15 January 2023
Accepted 12 February 2023
Available online 1 July 2023

Keywords:
Mask; Air permeability; Porosity; Aerosol containment; Pore size; COVID-19

ABSTRACT

At the end of 2019, the COVID-19 virus began to appear and quickly spread throughout the world. It transmits the infection to the respiratory tract by the transmission of pathogens within bioaerosols during speaking, coughing, and sneezing. Therefore, understanding the dynamics of aerosols plays an important role in developing mitigation strategies against droplet infections. Computational modeling, using fluid and computational dynamics, has become a useful feature in studying and visualizing the diffusion of micro-droplets that are difficult to reach using experimental methods. Through this study, the effects of using cloth face masks and social distancing, both recommended by the World Health Organization to the general public to avoid rapid transmission of COVID-19, were determined. This study made a comparison between different structural masks and the difference between social distancing with different porous masks at the droplet diameter during breathing from 0.5 µm to 2.5 µm. The results showed the effectiveness of wearing masks in reducing the risk of infection transmission. Also, with lower mask porosity, lower air permeability means higher filtration efficiency, trapping airborne particles more effectively, especially for small infection-carrying particle sizes, and, therefore, lowering the required social distancing. From the comparison, it is concluded that sample 6 has the highest efficiency of 82.9% compared to other samples (1, 2, 3, 4, and 5), which have efficiencies of 77.1%, 77.1%, 74.3%, 80.0%, and 65.7%, respectively.

1. Introduction

The coronavirus (COVID-19) pandemic spread rapidly across the world at the end of 2019. A respirator mask forms an airtight seal around the mouth and nose to protect the person from exposure to microorganisms such as bacteria, viruses, and fungi, as well as harmful airborne gases, as the World Health Organization recommends. Therefore, the mask filter must be able to filter out infectious microbes. Transmission of the COVID-19 virus has been assessed through practical experiments.

* *Corresponding author.*
E-mail address: fatma.abdelmordy@nis.sci.eg (Fatma A-M. Kassem)
https://doi.org/10.37934/cfdl.15.7.175193

It was concluded that the disease is spread by droplets during the exhalation of the patient through coughing, sneezing, and talking or direct communication with an infected human [1-2]. Bio-aerosol scattering is very important in the diffusion of this virus, and droplets with small sizes are harmful when compared with droplets with large sizes often created [3]. The World Health Organization (WHO) has confirmed the risk of airborne infection transmission by inhalation or ingestion by people around the patient.

Recently, COVID-19 has mutated, threatening many people with chronic diseases. Studies show that COVID-19 attacks males more compared to females and that the elderly from the age of 60 and above are mostly affected. As a result of what some studies have shown, the level of indoor air pollution can reach 2-5 times higher than outdoor air [4-5]. Therefore, it is recommended to wear medical/cloth masks and keep a social distance of about 1 m [6]. Although the surgical mask is able to filter bacteria and other infection particles (smaller than 0.1 μm) with an efficiency of more than 98%, it is not tight around the nose and mouth. Except that it provides very little protection from infection, it works efficiently for three to eight hours, depending on indoor air conditions such as humidity and temperature [7]. A particle mass consists of liquid droplets and small solid particles that are suspended in the air and vary in size, shape, surface area, and solubility. Particles with diameters less than 2.5 μm are often considered more dangerous than larger-sized particles because they can penetrate the deeper parts of a person's respiratory area [8]. WHO (World Health Organization) reports non-medical/clothes-to-mask's minimum performance in terms of filtration (minimum 70% solid particle filtration or droplet filtration) and breathability (maximum pressure difference of 0.6 mbar/cm^2. The WHO uses three parameters (initial filtration efficiency, initial pressure drop (Pa), and filtering quality factor (FQF)) to evaluate the filtration efficiency of cloth masks [9].

However, most of the studies were conducted to assess risk-using populations. It is explained that the use of face masks at the population level could delay the COVID-19 pandemic. In addition, the effect of wearing masks in enclosed spaces such as airplanes and homes has been studied [10, 11]. In addition to the velocity and pressure distribution of fluid across the mask filtration layer N95 [12]. These studies provided evidence that masks can contribute to the prevention and reduction of infection transmission [13]. For areas where it is difficult to maintain a 6-foot social distance and that are frequented by people to avoid cross-infection (for example, supermarkets and pharmacies), the Centers for Disease Control and Prevention recommend wearing a face mask. In addition, the Centers for Disease Control recommend the use of simple cloth face-covering masks to slow and reduce the spread of the virus from personnel who may be infectious without knowing it [14]. The transmission of airborne infection depends on airflow distributions from the ventilation system [15].

Therefore, this paper describes the performance evaluation of various structural masks. The main goal of the solutions was to get rid of the epidemic and protect the medical staff in hospitals. In this study, several masks will be tested and evaluated experimentally and numerically under different conditions to assess factors concerning the selection of materials and related layers in the manufacturing of commercial fabric-cloth masks, which may help both manufacturers and health establishments in evaluating their efficiency.

2. Experimental Work

2.1 Room Design and Flow Measurement

The experiments were carried out in a full-size room. The length and width of the room are 2.0 m and 2.0 m, respectively, and their height is 2.0 m. It consists of one air exhaust and one air inlet location, as shown in Figure 1. For the room, the dimensions of the inlet grill are 0.60 (L) and 0.20 (H), and the outlet opening is 0.35 (L), and 0.35 (H). The isolation room is illuminated by a lamp with

a power of 18 W/m^2. The patient was lying on a bed with and without wearing a mask at a height of 0.7 m from the floor. During the experiments, the ventilation system supplied air at 21^{o}C± 0.035^{o}C and volume flow rate at inlet 216 m^3/hr. To reach stable conditions, the room was allowed to equilibrate for a half hour before the measurements were taken. In the experiments, the patient's manikin is exhaled through the nose according to the sinusoidal velocity Eq. (1). The flow rate during the exhale stroke is controlled using a Rota-meter, solenoid valve, and timer, as shown in Figure 2. The nose consists of two holes with a diameter of 6 mm. The respiratory minute volume is (9.0 ± 0.35 l/min) and the breathing frequency is 15 min^{-1}. The trace gas concentration is measured continuously using an air quality sensor ranging from 400 ppm to 29,206 ppm at measurement locations. Two sampling points (P1 and P3) were installed inside the room around the patient bed at 1.0 m from floor level to assess the CO_2 concentration. One of the sampling points (P2) was located around the bed, 1.4 m from floor level, at the same level as the healthcare worker [16, 17].

$$v = 1.99 \sin\left(\frac{\pi}{2} t\right) \tag{1}$$

(a) Without wearing a mask (b) With wearing a mask

Fig. 1. Measuring points location

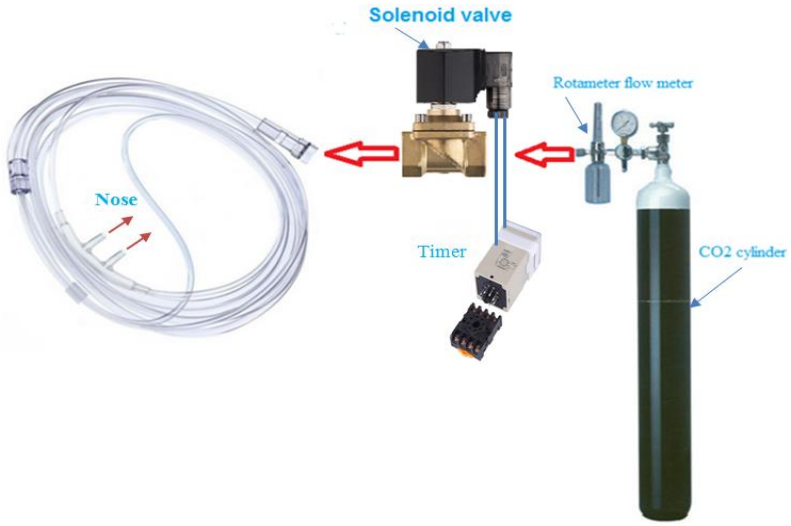

Fig. 2. Circuit of exhaled stroke

2.2 Mask Specification

Wearing a face mask has become an effective way to reduce the transmission of COVID-19. In this work, the effectiveness of the mask was tested in different structures of the face without a mask and the face with a mask. In this study, six samples of masks of different compositions (three layers) were used. Mask thickness is an important factor in calculating the porosity, the minimum, average, and maximum pore size, and the number of pores using a Porometer, as shown in Figure 3(a), which is measured using a digital thickness gauge, as shown in Figure 3(b). The air permeability of a non-woven mask at the pressure of 104 Pa.

This study focuses on determining the mechanical and physical properties of commercially available disposable 3-layer masks.

(a) Porometer device (b) Digital thickness gauge

Fig. 3. Porosity measuring test rig

2.3 Mask structure

This study uses six mask samples with 3 layers. Two samples (1 and 2) are medical masks, and samples (3, 4, 5, and 6) are nonwoven masks, as shown in Figure 4. Table 1 explains the lowest bubble pressure and bubble flow rate to open the pores with several repeated times (n=3). It is noted that the pores of sample 6 opened at the smallest pressure (0.01 bar) compared with sample 1 (0.05 bar).

This is due to the mean pore diameters of 56.7 µm and 12.5 µm, respectively. The pore diameter for sample 6 is four times compared that the sample 1. Thus, it takes almost four times the pressure to open the pores. Table 2 summarizes the basic characteristics of the masks. Mask sample 3 shows the highest values for thickness and total weight. Sample 2 is the thinnest and lightest mask, and Table 3 explains the mask material description.

Table 1
The initial condition of the different masks (mean ± SD, n=3)

Sample	1	2	3	4	5	6	
Bubble point pressure (bar)	0.0511± 0.0026	0.0292± 0.00035	0.0238± 0.001586	0.0178± 0.00047	0.0206± 0.000601	0.0102±	0.000033
Bubble point flow rate (l/m)	0.0012± 0.00062	0.0016± 0.00032	0.0046± 0.00089	0.0029± 0.001419	0.0084± 0.002136	0.0009±	0.000754

Table 2
Specification of the masks (mean ± SD, n=3)

Sample	Minimum pore size (µm)	Mean pore size (µm)	Maximum pore size (µm)	Total weight of 3 layers (g/m2)	Viscous resistance (inverse absolute permeability) (1/m)	Thickness mask (µm)	Pores Number
1	7.9632± 1.6583	10.0022± 1.8624	12.5196± 1.9116	86.289	6.648×10^{10}	421± 0.971	1.25×10^{6}
2	13.2231± 1.8130	16.5387± 1.7023	21.9178± 1.654	51.908	2.727×10^{10}	245± 0.971	1.37×10^{5}
3	11.9649± 1.884	14.8978± 2.397	26.8569± 3.588	492.490	5.413×10^{10}	987±0.849	2.26×10^{5}
4	20.813± 4.237	28.265± 1.591	36.0563± 2.391	439.950	9.08×10^{9}	725±0.849	1.89×10^{4}
5	18.2492± 2.9114	21.6304± 2.0895	31.0982± 2.5353	372.300	6.00×10^{9}	660±0.971	4.36×10^{4}
6	62.9921± 1.638	59.2365± 1.566	56.7376± 1.565	364.256	3.10×10^{9}	623±0.971	2.20×10^{3}

Table 3
Mask structures

Sample	Description
1	100%polypropylene nonwoven material High bacteria filtration (3 layers: BFE>99% Manufacture (CHEMI Pharma medical)
2	Polyethylene out-layer and soft inner-facing fabric gamma irradiation with a sterility assurance level of 10-6 Excellent bacteria and filtration efficiency BFE: 94.1% at 3 microns and 89.3% at 0.1 microns. Manufacture (medic Egypt for medical clothes)
3	Mask consists of 3 layer Outer-layer 60% polyester fabric and 40% cotton and antimicrobial treatment. Inner layer Water repellent 100% cotton. The layer adjacent to the face is 100% cotton. Manufacture: Mary Wei. (PTM)
4	Mask consists of 3 layer Outer-layer 60% polyester fabric and 40% cotton and antimicrobial treatment. Inner layer Water repellent 100% cotton. The layer adjacent to the face is 100% cotton. Manufacture: Eng. Mostafa
5	Mask consists of 3 layer Outer-layer 60% polyester fabric and 40% cotton and antimicrobial treatment. Inner layer Water repellent 100% cotton. The layer adjacent to the face is 100% cotton. Manufacture: Eng. Mostafa
6	Mask consists of 3 layer Outer-layer 60% polyester fabric and 40% cotton and antimicrobial treatment. Inner layer Water repellent 100% cotton. The layer adjacent to the face is 100% cotton. Manufacture: Hesn Textiles

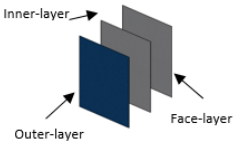

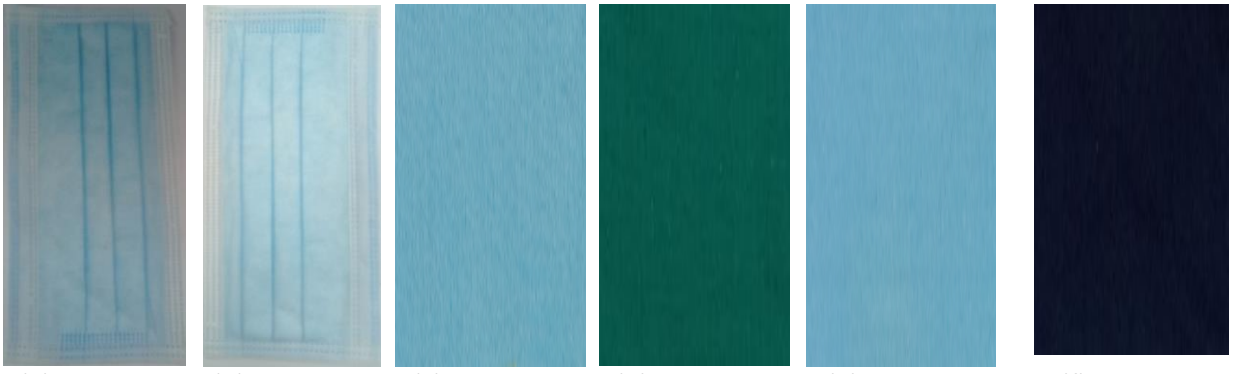

(a) Sample 1 (b) Sample 2 (c) Sample 3 (d) Sample 4 (e) Sample 5 (f) Sample 6

Fig. 4. Mask samples

3. Computational Fluid Dynamics Simulation

3.1 Design Models and Grid Independence Test

This hybrid scheme has maintained a better mesh quality. The results of the grid independence check over three grid resolutions are presented in Figures 5 and 6. V refers to the velocity magnitude of room air observed at a specific line, and Y is the height of room air monitored at the specific line. The velocity at the monitored points in the case of 1,657,317 cells was very close to that of the

1,734,126 cells. Moreover, the relative error of the average room air velocity between cases 1 and 2, cases 1 and 3, and cases 2 and 3 reported -1.91%, -3.32%, and -1.44%, respectively. It could be concluded that the grid system reached an independent solution. Therefore, the grid density of 1,989,192 cells was found to be sufficient and applied in the ongoing study.

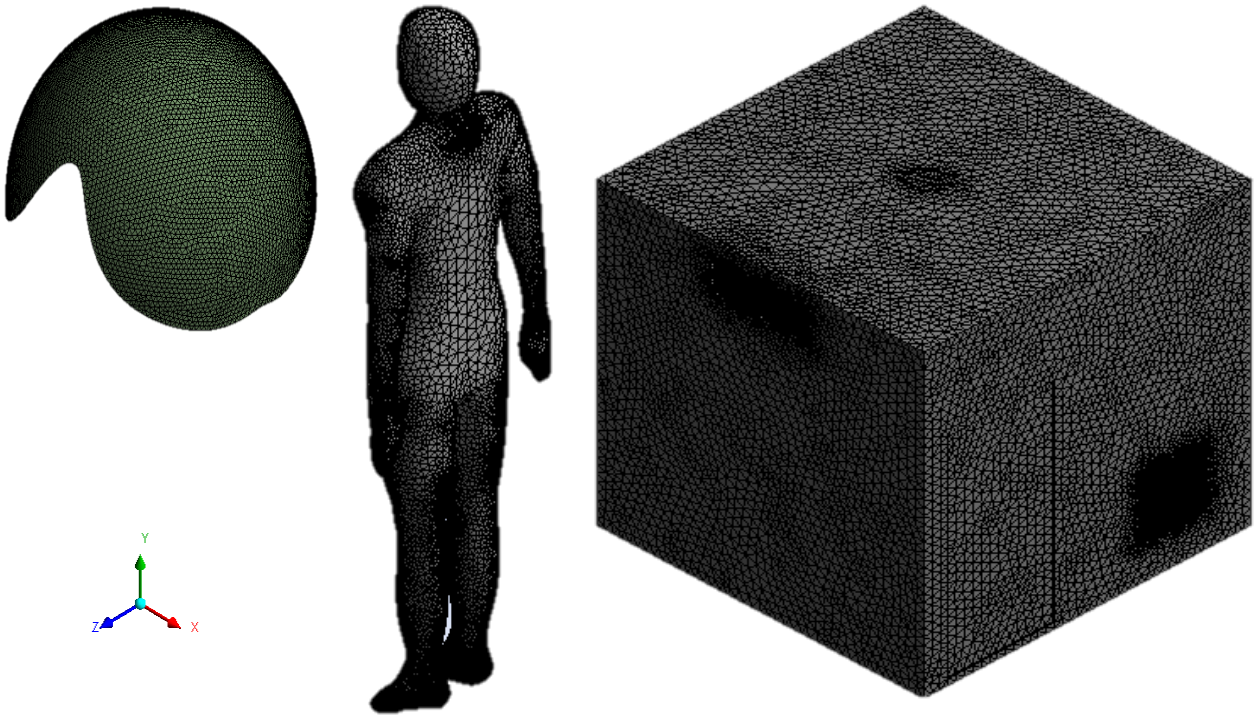

(a) Mask (b) Healthcare worker (c) Isolation room

Fig. 5. Mesh configuration

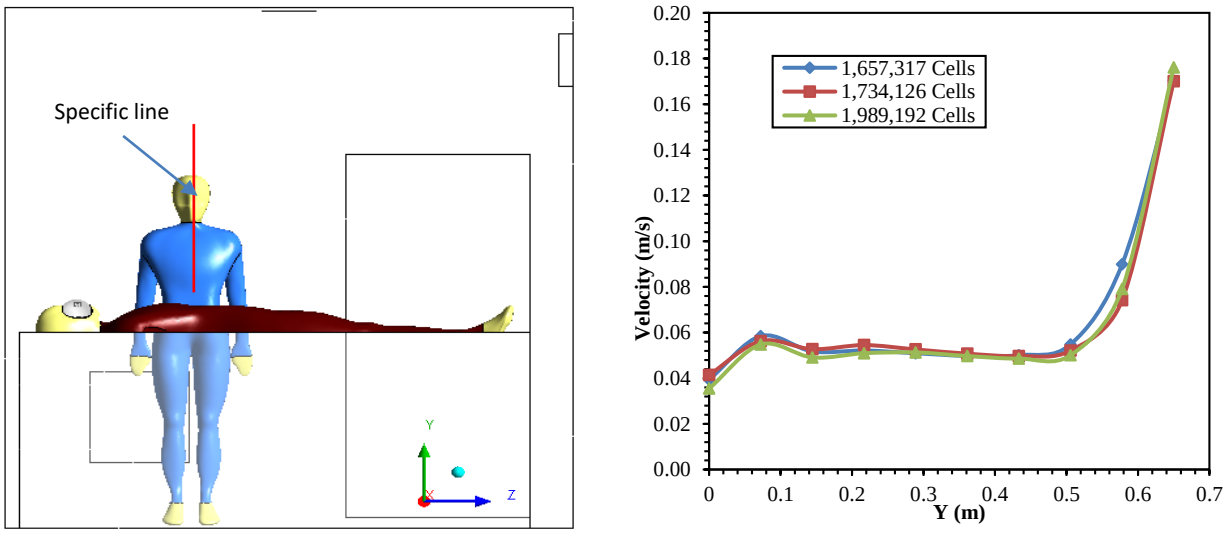

(a) Position of significant line (b) Mesh sensitivity analyses at the significant line from the healthcare

Fig. 6. Grid-independent test

3.2 Boundary Conditions

The transient simulation of airflow in the room was carried out based on the pressure. The simulations were carried out using ANSYS Fluent software (V-16). The two-equation k-ε RNG turbulence model with the standard wall functions was selected by [16] to be robust and stable for single-phase airflows in indoor environments. Pressure-velocity coupling was achieved using the coupled scheme. The second-order upwind scheme was used for the discretization of pressure, momentum, turbulent kinetic energy, and dissipation rate. Convergence was considered to have been reached when the residuals were less than 10^{-4} for the flow variables (continuity, x-velocity, y-velocity, and z-velocity, k, and ε) while the energy equation was less than 10^{-6}. Each transient simulation was performed for 50 s with a time-step of 0.1 s and 27 ACH (Air Change per Hour is the ratio of volume flow rate at inlet grill (m^3⁄hr) to room volume (m^3)). The details of the boundary condition are shown in Table 4 [16].

Table 4
CFD solution setup settings

Condition	Type	Value
Steady/transient	Steady (RANS)	
Turbulence model	K-ε	
Dispersed phase model	DPM: Injection	Velocity: 0 m/s Flow rate: $1 \times 10^{-5} kg/s$ Particle Size: 0.5–2.5 µm, median 1 µm Diameter distribution: rosin-rammler logarithmic
Supply air	Velocity inlet Discrete phase: escape	Velocity: 0.5 m/s Temperature: 295 °K
Exhaust air	Pressure outlet Discrete phase: escape	Pressure: 0 Pa Temperature: 298 °K
Nose patient	Velocity inlet Discrete phase: escape	V=1.99×sin((3.14/2)×t) Temperature: 300 °K
Patient, healthcare worker, and bed	Wall	Adiabatic
Coupled scheme	Pressure-velocity coupling	
Convergence residuals	10^{-4} except energy equation 10^{-6}	

4. Results and Discussion

4.1 Validation Between Experimental Work and Numerical Model

The mean of carbon dioxide CO_2 concentration for the experimental results and computational fluid dynamic simulation is shown in Figure 7. The CFD data agree very well with experimentally measured concentrations of airborne particles at different measuring points from P1 to P3. The average error between the experimental measurement and CFD simulation is nearly 11%. The maximum evaluated uncertainty from the measurement is ± 2.0 ppm.

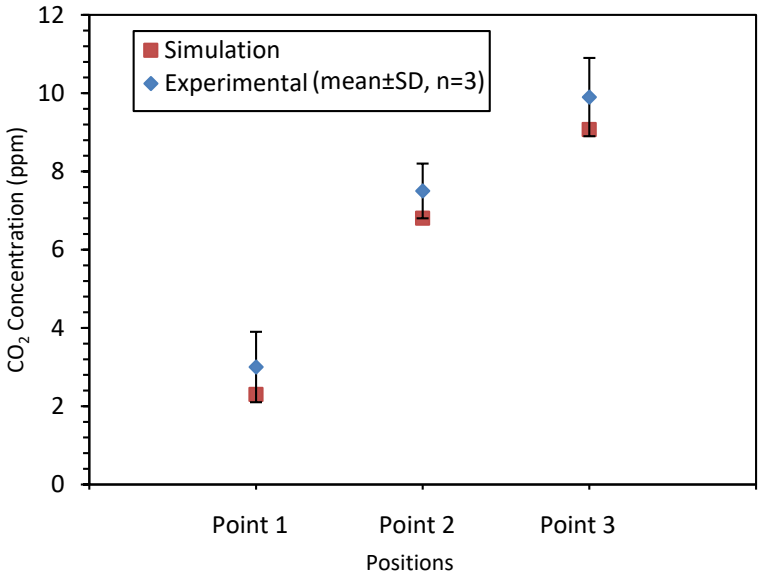

Fig. 7. Comparison between experimental and simulation results

4.2 CO_2 Concentration

The mean carbon dioxide concentration inside the room was measured using three measuring points (P1, P2, and P3) by an air quality sensor connected to a computerized system. The average reference value for CO_2 inside the room, before the experiment was conducted and before CO_2 was injected as an airborne gas, was 400 ppm. The tracer gas (CO_2) was used to monitor how concentrations were removed. Figure 8 shows the air in the indoor environment when the patient with and without wearing a mask. The pressure inside the room was 0.3 Pa at 27 ACH. For the patient without a mask and ACH 27, the exhalation spread within the room but was moving in the direction of the exhaust, as shown in curve P4.

For the patient without a mask and ACH 12, indoor air was also mixed and slowly diffused into the room. This is due to the thermal buoyancy effects, which cause airborne contaminants to spread into the room and take a long time to reach the exhaust. But when wearing a patient mask, the exhalation spreads slowly into the room due to the resistance of the mask and the pressure drop around the mask. Exhalation moves slowly, with less concentration and less distance compared to wearing a mask incorrectly.

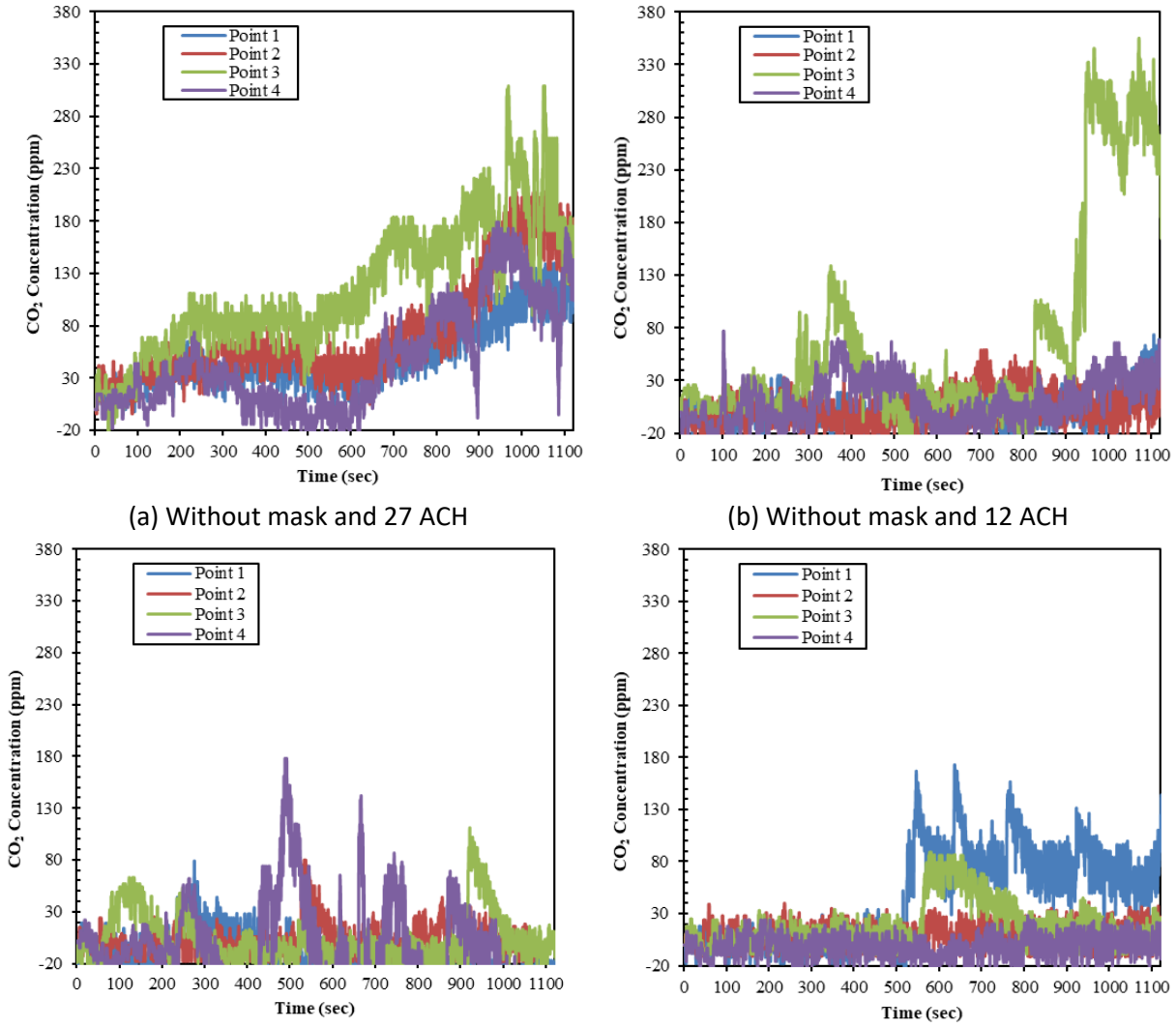

(a) Without mask and 27 ACH

(b) Without mask and 12 ACH

(c) With mask and 27 ACH (Sample 1)

(d) With mask and 12 ACH (Sample 1)

Fig. 8. Experimental results for CO_2 concentration with and without mask at different ACH

4.3 Air Permeability with Different Masks

The porosity, air permeability, and mean pore size values of various masks are given in Figure 9. It is observed that the air permeability of the masks in samples 3, 4, and 5 was lower than that of the masks in samples 1, 2, and 6. The air permeability of the mask is important in terms of providing high filtering capacity [18] and breathing capability. Besides, it should prevent the entry and exit of microorganisms during inhalation and exhalation.

The air permeability of nonwoven fabrics is affected by several factors, such as porosity [19], weight, thickness, fiber diameter, and fiber distribution in the nonwoven web [20, 21]. It is revealed that the melt-blown layers are the most effective layers in blocking, and they have lower porosity than the spun-bonded layers. Also, the melt-blown layers have a compact structure compared to spun-bonded ones [19]. The calculated surface porosity values for mask samples 4, 5, and 6 are lower than those for mask samples 1, 2, and 3 due to lower air permeability. The air permeability of mask sample 6 is observed to be higher than that of mask sample 5, although the porosity of sample 5 is higher than 6. The reason is that the mean pore size of mask sample 6 is higher than that of mask sample 5.

The lower thickness and lower total weight values of sample 2 are also responsible for the highest air permeability. Low air permeability means high filtration efficiency as airborne particles are trapped more effectively [18].

The air permeability of samples 1 to 6 varies from 60 to 120 l/m^2/s in the combination of three layers at an air pressure of 105 Pa. The differences in the air permeability and porosity of the samples may be due to the differences in the pore sizes and the number of opening pores of these samples, as shown in Figure 9b. Although the cumulative number of pores is greater in sample 1, the air permeability is higher in sample 2. This is due to the higher mean pore size in sample 2 compared to sample 1.

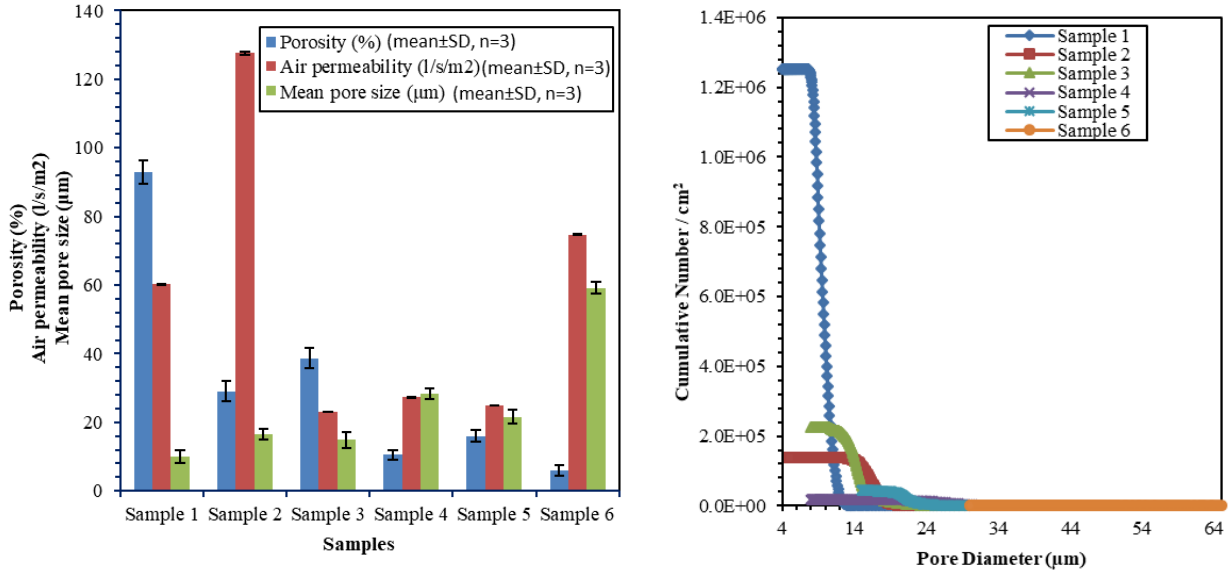

(a) Porosity, air permeability, and mean pore size for different mask

(b) Cumulative number per area vs pore diameter

Fig. 9. Properties of various structure masks

4.4 Aerosol Droplets Tracking Diameter

The aerosol droplet tracking diameter for different structure masks is shown in Figure 10. It is observed that the number of aerosol droplets exiting from mask sample 6 is less than that of mask samples 1, 2, 3, 4, and 5 due to the low porosity and cumulative number of pores per area for the sample. Conversely, Sample 1 is higher than the number of aerosol droplets leaving the mask due to the high porosity and the cumulative number of pores per area. The number of aerosol droplets leaving the mask depends on the porosity of the mask and the cumulative number of pores.

4.5 Droplet Residence Time and Social Distance

Figure 11 presents the time residence of the dispersed aerosol droplets after 50.0 s from the patient at 27 ACH with different mask samples. It is noted that the velocity field for samples (a, b, and c) is remarkably different from the rest of samples (d) to (i).

When the air change per hour increases from 2.7 to 27 ACH, the aerosol droplets move towards the exhaust opening and travel less distance due to the increased pressure difference inside the room and the exhaust opening.

As the mask porosity increases, exit droplet resistance decreases. The aerosol droplets move in the direction of the exhaust due to the generated air flow by the mask becoming more robust. This

will help reduce the risk of healthcare workers' exposure to harmful aerosol droplets. With a constant ACH, it is noticed that the social distance when wearing the mask is reduced to about one-third compared to when not wearing the mask, as shown in Table 5. Additionally, the residence time for large particles decreases, while for small particles it increases.

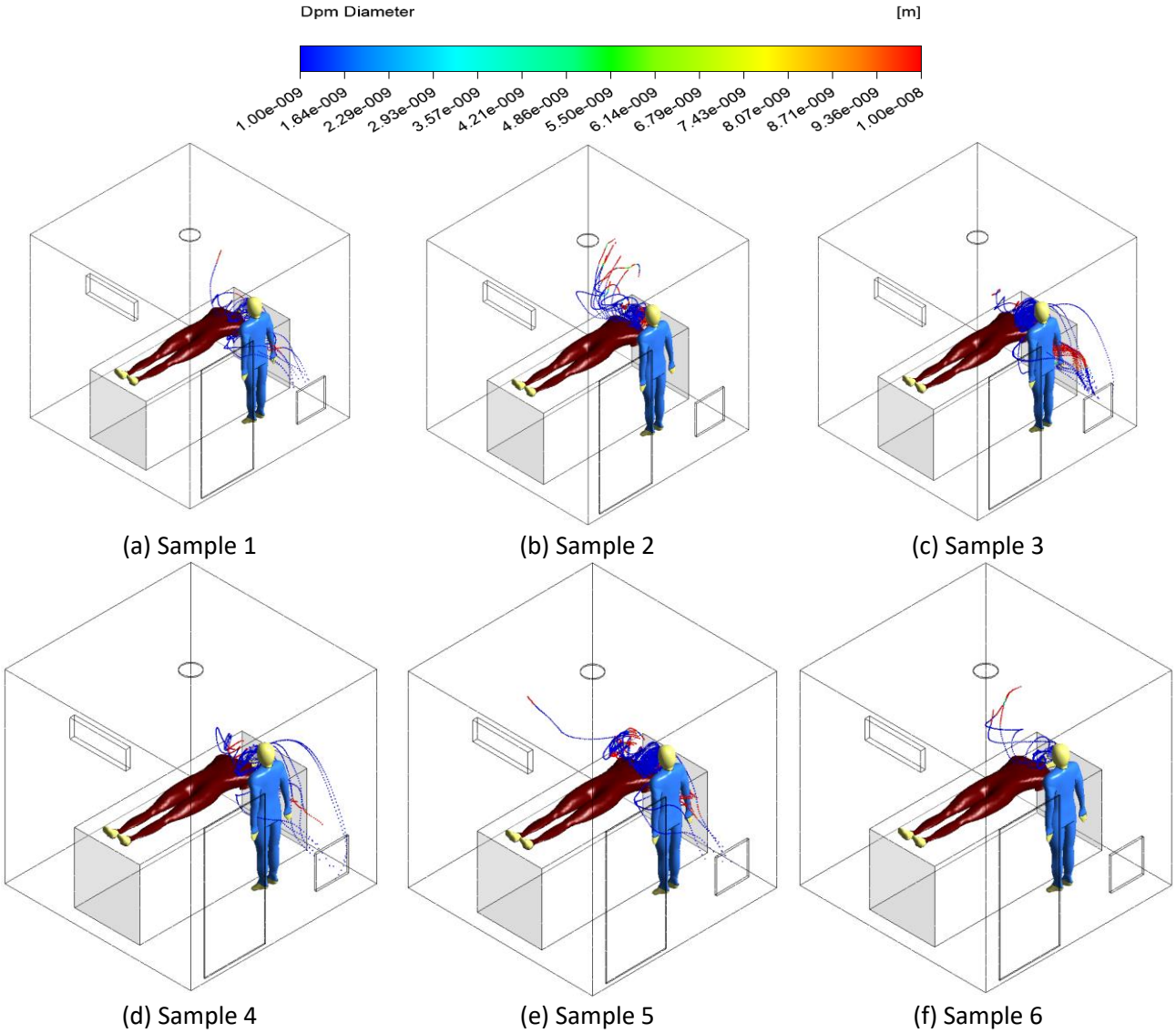

(a) Sample 1 (b) Sample 2 (c) Sample 3

(d) Sample 4 (e) Sample 5 (f) Sample 6

Fig. 10. Aerosol droplets tracking diameter with various mask samples and 27ACH

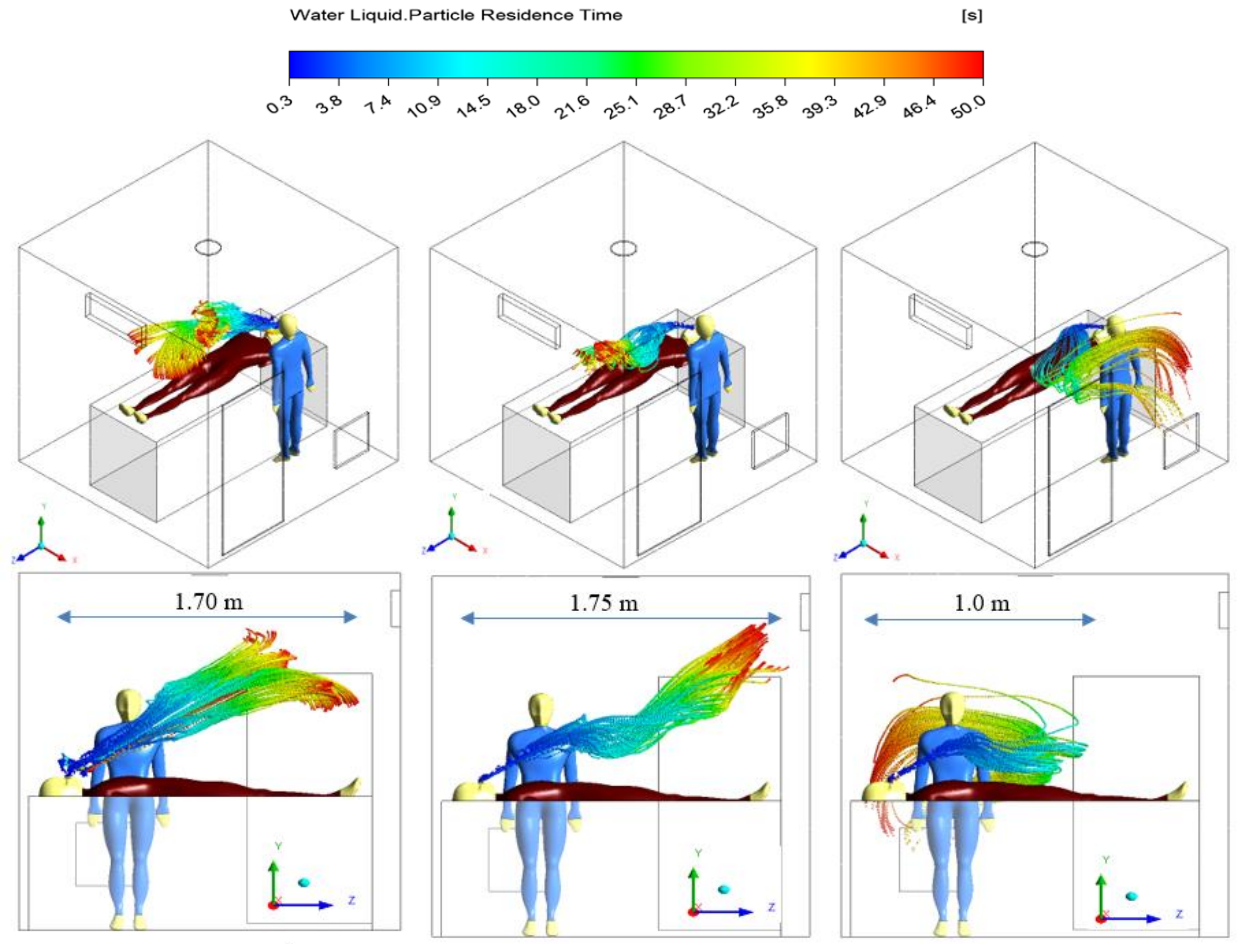

(a) Without mask ACH= 2.7 (b) Without mask ACH= 12 (c) Without mask ACH= 27

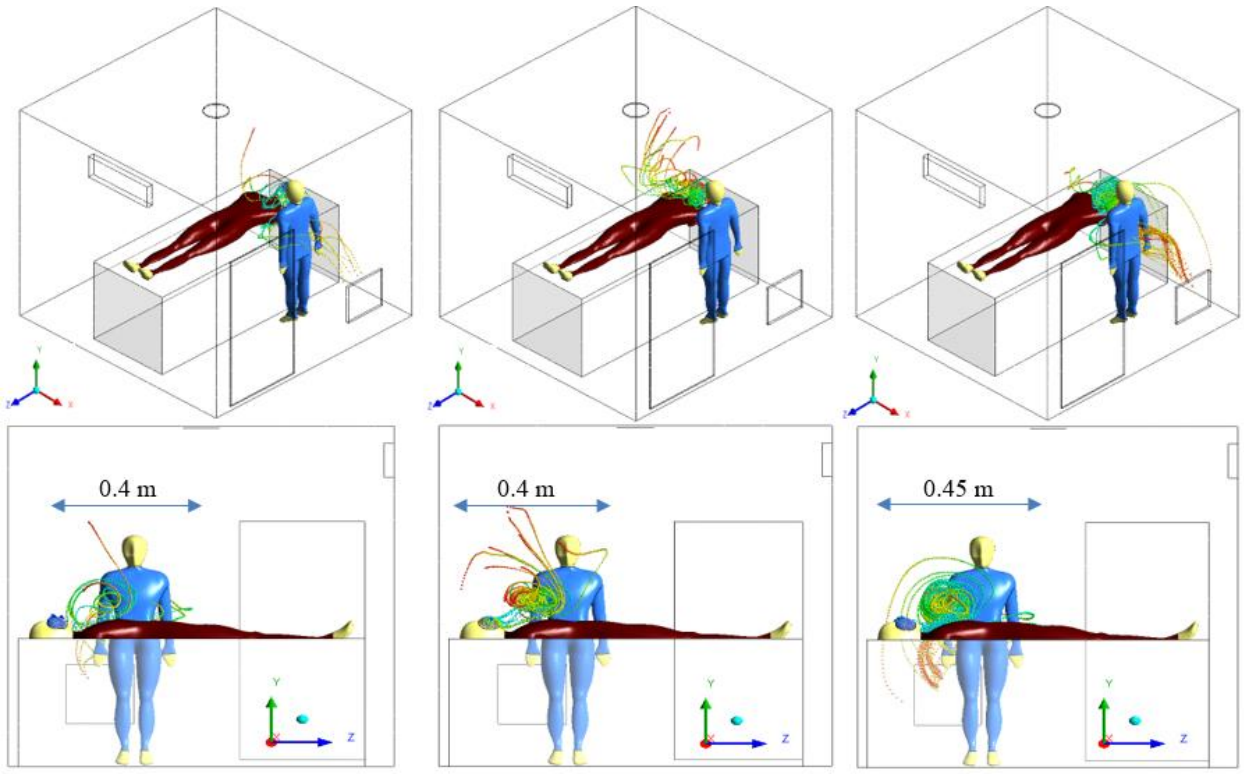

(d) Sample 1 (e) Sample 2 (f) Sample 3

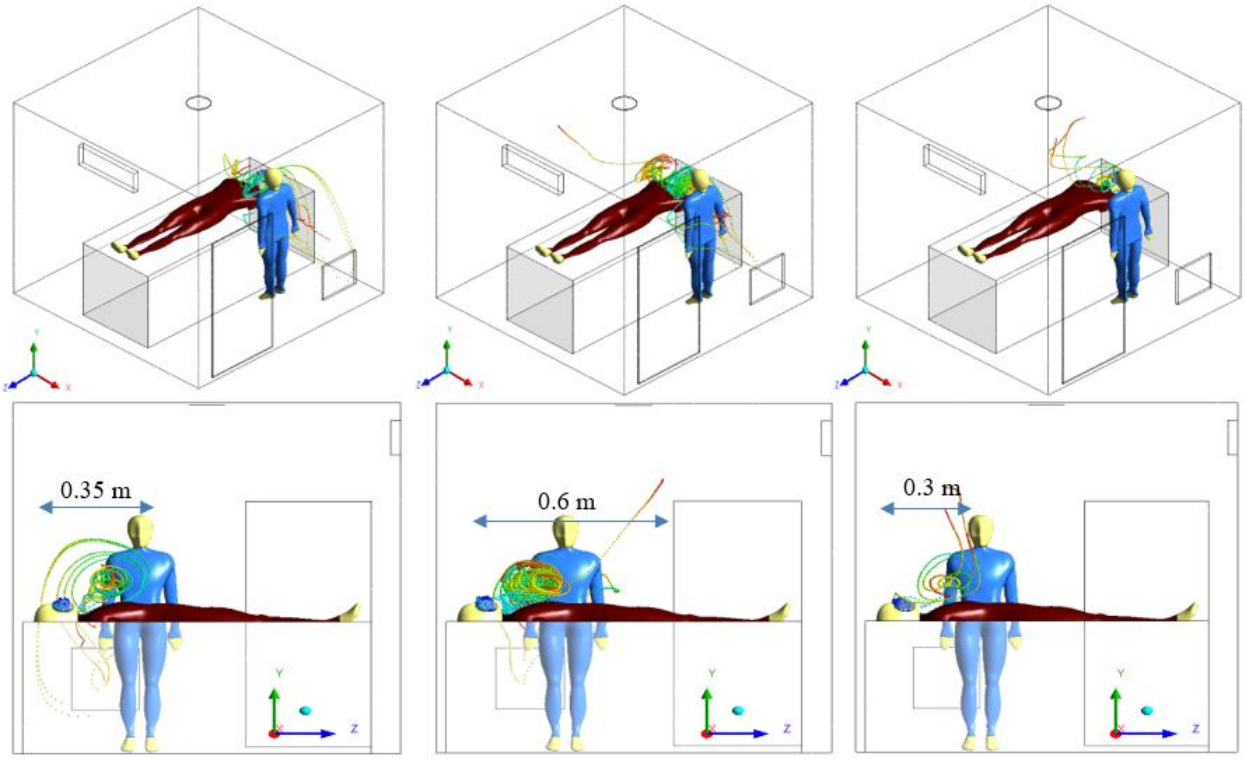

Fig. 11. Numerical results for water droplet diameter with various strategies and 27ACH

4.6 Wearing Mask Incorrectly

In the case of incorrectly wearing a mask, the aerosol droplets seep through the gaps between the face and mask in large numbers, as shown in Figure 12. They move in the direction of gravity and the direction of the exhaust opening due to the difference in pressure (pressure inside room is 0.3 Pa and pressure at the exhaust is 0 Pa). This suggests that gravity and pressure differences play an important role in the carriage of particles smaller than 10 nm. Thus, the risk of infection of healthcare workers increases because a greater number of aerosol droplets are released into the room compared to when wearing a mask correctly. Therefore, the mask must be worn correctly to reduce the risk of infection.

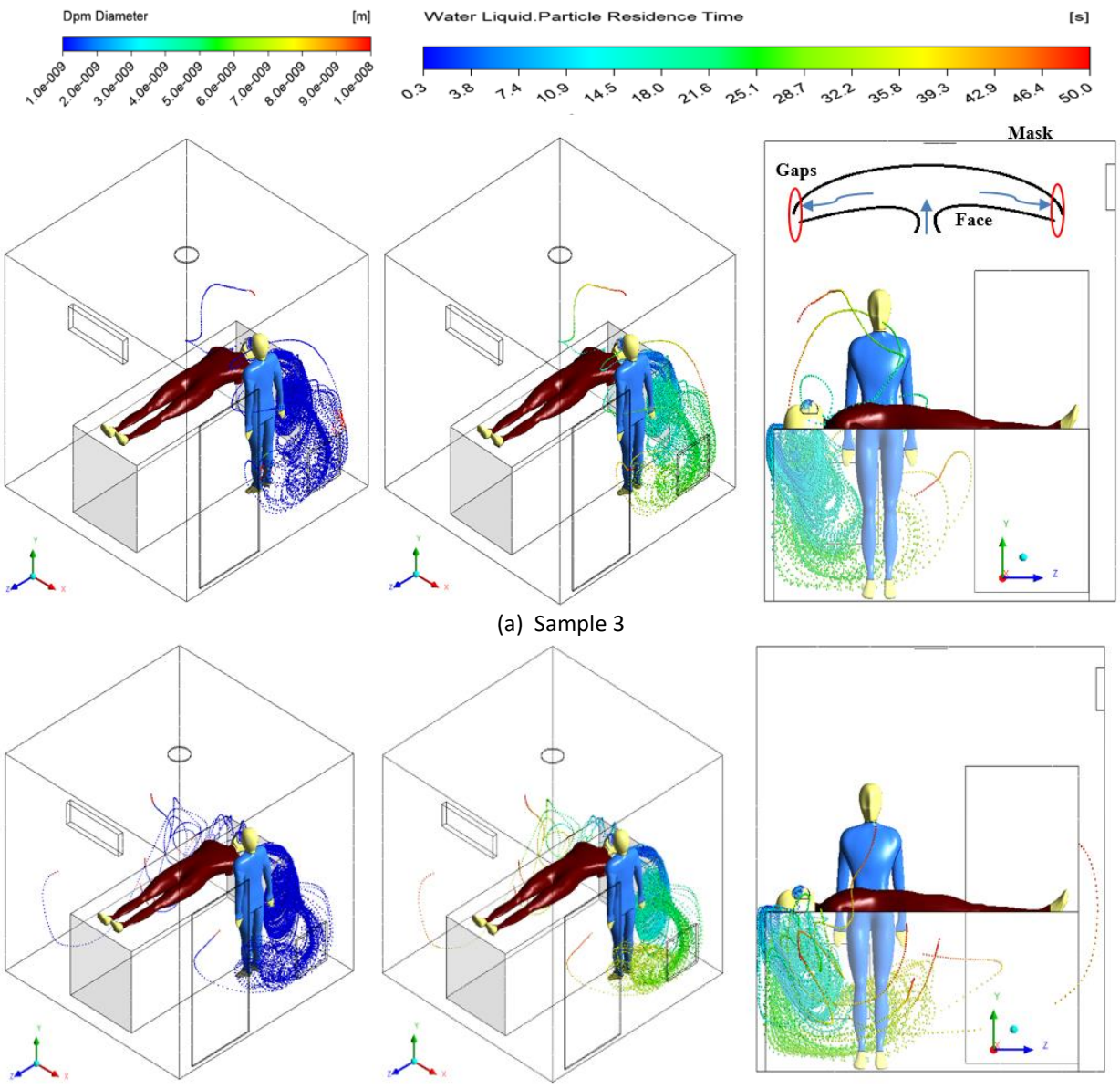

(a) Sample 3

(b) Sample 4

Fig. 12. Water aerosol diameter and time residence in case wearing mask incorrectly

4.7 Effectiveness of the Mask Samples

A mask's filter efficiency is used to compare many devices that are different in structure, materials, and manufacturing. The efficiency of the mask μ is calculated according to Eq. (2), as shown in Figure 13, where u and d are the water droplet concentrations upstream and downstream of the mask, respectively. The commercial mask efficiency ranges from 65.7% to 82.9%, while the medical mask efficiency is 77.1%. According to Ref. [9], all samples conform except sample 5, which was out of range because the efficiency was lower than the recommended value of 70%.

$$\mu\ (\%) = \left(\frac{C_u - C_d}{C_u}\right) \times 100 \tag{2}$$

Table 5
Comparisons with related previous work

Type state	Droplet diameter (μm)	ACH/ Velocity	Social distance (m)	Time residence (sec)	Porosity %	Ref(s).
Exhaled breathing	10	-	≤ 1	300	-	[22-27]
	1	-	≥ 2	30,000	-	[22-27]
Violent exhalation	< 200		0.7	0.34	-	[28, 29]
Exhaled breath (No wearing mask)	-	16	0.68	-	-	[30, 31]
Exhaled breath (No wearing mask)	0.5 - 2.5	12	1.75	50	-	Present study
Exhaled breath (No wearing mask)	0.5 - 2.5	27	1	50	-	Present study
Exhaled breath (wearing mask)	0.5 - 2.5	27	0.4	50	93	Present study
Exhaled breath (wearing mask)	0.5 - 2.5	27	0.4	50	29	Present study
Exhaled breath (wearing mask)	0.5 - 2.5	27	0.45	50	38	Present study
Exhaled breath (wearing mask)	0.5 - 2.5	27	0.35	50	11	Present study
Exhaled breath (wearing mask)	0.5 - 2.5	27	0.6	50	16	Present study
Exhaled breath (wearing mask)	0.5 - 2.5	27	0.3	50	6	Present study

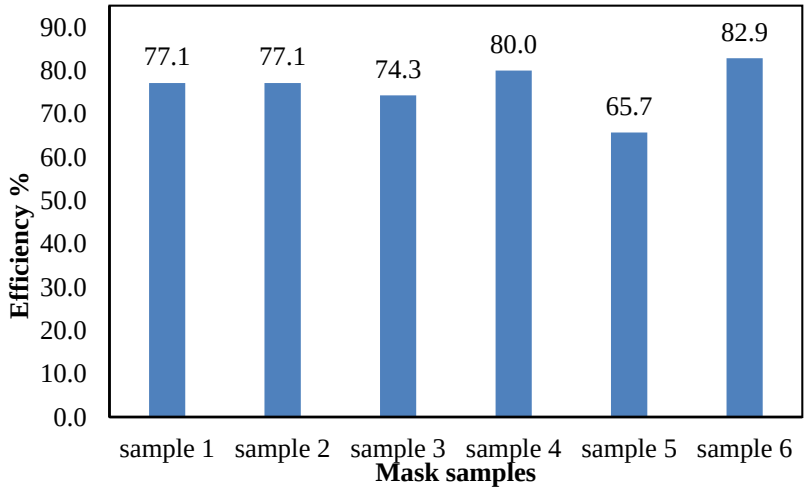

Fig. 13. Efficiency with different mask samples

5. Conclusion

This study aims to test the commercial masks available on the market to find out the extent of their ability to prevent the transmission of infection from one person to another. It was concluded that the porosity of the mask and the number of pores in the mask play an important role in avoiding the transmission of infection at low social distances. In addition, the proper way of wearing the mask had significant effects on the results. In this study, the aerosol droplet of exhaled contaminants generated by human breathing in a room using different structure masks is numerically examined. Looking at the results obtained, the following conclusions can be drawn:

i) Good agreement was achieved between the experimental and simulation results. This is evidence of the compatibility of the boundary conditions used in the computational work.
ii) Wearing a mask slows down the movement of infection-carrying droplet particles.
iii) Wearing the mask correctly greatly reduces the spread of infection with aerosol droplets. The number of aerosol droplets leaving the mask depends on its porosity and the cumulative number of pores in addition to wearing the mask correctly.
iv) The number of droplets leaving sample 6 is less compared to sample 3 because of its lower air permeability and fewer pores.
v) Social distance depends on air change per hour as the resulting contour reduces the social distance from 1.75 m to 1 m at 12 to 27 ACH.
vi) Although sample 6 gives the least social distance, it is not recommended to use this type because of the small value of the porosity of the sample. In the case of using these samples, this may negatively affect the person's health as a result of inhaling part of the carbon dioxide during the exhalation process due to the mask's inability to get rid of the carbon dioxide.
vii) At a constant ACH, it was observed that the social distance when wearing a mask is reduced to about one-third compared to when not wearing a mask.
viii) All samples are conformant according to [9], except sample 5, where the efficiency is less than 70%. This is evidence that it is not suitable as a face covering to protect against any virus.

References

[1] Van Doremalen, Neeltje, Trenton Bushmaker, Dylan H. Morris, Myndi G. Holbrook, Amandine Gamble, Brandi N. Williamson, Azaibi Tamin et al. "Aerosol and surface stability of SARS-CoV-2 as compared with SARS-CoV-1." *New England journal of medicine* 382, no. 16 (2020): 1564-1567. https://doi: 10.1056/NEJMc2004973

[2] Induri, Sri Nitya Reddy, Yunah Caroline Chun, Joonmo Christopher Chun, Kenneth E. Fleisher, Robert S. Glickman, Fangxi Xu, Efthimia Ioannidou, Xin Li, and Deepak Saxena. "Protective measures against COVID-19: Dental practice and infection control." In *Healthcare*, vol. 9, no. 6, p. 679. MDPI, 2021. https://doi.org/10.3390/healthcare9060679

[3] Liu, Yuan, Zhi Ning, Yu Chen, Ming Guo, Yingle Liu, Nirmal Kumar Gali, Li Sun et al. "Aerodynamic analysis of SARS-CoV-2 in two Wuhan hospitals." *Nature* 582, no. 7813 (2020): 557-560. https://doi.org/10.1038/s41586-020-2271-3

[4] Ahad, Nor Aishah, Friday Zinzendoff Okwonu, and Yik Siong Pang. "COVID-19 Outbreak in Malaysia: Investigation on Fatality Cases." *Journal of Advanced Research in Applied Sciences and Engineering Technology* 20, no. 1 (2020): 1-10. https://doi.org/10.37934/araset.20.1.110

[5] Tan, Huiyi, Keng Yinn Wong, Hong Yee Kek, Kee Quen Lee, Haslinda Mohamed Kamar, Wai Shin Ho, Hooi Siang Kang et al. "Small-scale botanical in enhancing indoor air quality: A bibliometric analysis (2011-2020) and short review." *Progress in Energy and Environment* 19 (2022): 13-37.. https://doi.org/10.37934/progee.19.1.1337

[6] World Health Organization, (2020. Transmission of SARS-CoV-2: implications for infection prevention precautions: scientific brief, 09 July 2020. No. WHO/2019-nCoV/Sci_Brief/Transmission_modes/2020.3. *World Health Organization*, 2020.

[7] Goh, Yihui, Benjamin YQ Tan, Chandra Bhartendu, Jonathan JY Ong, and Vijay K. Sharma. "The face mask: How a real protection becomes a psychological symbol during Covid-19?." *Brain, behavior, and immunity* 88 (2020): 1-5. https://doi.org/10.1016/j.bbi.2020.05.060

[8] Pacitto, Antonio, Fulvio Amato, Apostolos Salmatonidis, Teresa Moreno, Andrés Alastuey, Cristina Reche, Giorgio Buonanno, C. Benito, and Xavier Querol. "Effectiveness of commercial face masks to reduce personal PM exposure." *Science of the total environment* 650 (2019): 1582-1590. https://doi.org/10.1016/j.scitotenv.2018.09.109

[9] Santarsiero, A., M. Giustini, F. Quadrini, D. D'Alessandro, and G. M. Fara. "Effectiveness of face masks for the population." *Ann Ig* 33, no. 4 (2021): 347-59. https://doi:10.7416/ai.2020.2390

[10] Brienen, Nicole CJ, Aura Timen, Jacco Wallinga, Jim E. Van Steenbergen, and Peter FM Teunis. "The effect of mask use on the spread of influenza during a pandemic." *Risk Analysis: An International Journal* 30, no. 8 (2010): 1210-1218. https://doi.org/10.1111/j.1539-6924.2010.01428.x

[11] Zhang, Lijie, Zhibin Peng, Jianming Ou, Guang Zeng, Robert E. Fontaine, Mingbin Liu, Fuqiang Cui et al. "Protection by face masks against influenza A (H1N1) pdm09 virus on trans-Pacific passenger aircraft, 2009." *Emerging infectious diseases* 19, no. 9 (2013): 1403. https://doi: 10.3201/eid1909.121765

[12] Harolanuar, Muhammad Nur Hanafi, Nurul Fitriah Nasir, Hanis Zakaria, and Ishkrizat Taib. "Analysis of Fluid Flow on the N95 Facepiece Filtration Layers." *Journal of Advanced Research in Fluid Mechanics and Thermal Sciences* 100, no. 1 (2022): 172-180. https://doi.org/10.37934/arfmts.100.1.172180.

[13] Larson, Elaine L., Yu-Hui Ferng, Jennifer Wong-McLoughlin, Shuang Wang, Michael Haber, and Stephen S. Morse. "Impact of non-pharmaceutical interventions on URIs and influenza in crowded, urban households." *Public health reports* 125, no. 2 (2010): 178-191. https://doi.org/10.1177/003335491012500206.

[14] Coclite, Daniela, Antonello Napoletano, Silvia Gianola, Andrea Del Monaco, Daniela D'Angelo, Alice Fauci, Laura Iacorossi et al. "Face mask use in the community for reducing the spread of COVID-19: a systematic review." *Frontiers in medicine* 7 (2021): 594269. https://doi.org/10.3389/fmed.2020.594269

[15] Kalliomäki, Petri, Pekka Saarinen, Julian W. Tang, and Hannu Koskela. "Airflow patterns through single hinged and sliding doors in hospital isolation rooms." *International Journal of Ventilation* 14, no. 2 (2015): 111-126. https://doi.org/10.1080/14733315.2015.11684074

[16] Kassem, Fatma AbdelMordy, Ahmed Farouk AbdelGawad, Ali Elsayed Abuel-Ezz, Mofreh Melad Nassief, and Mohamed Adel. "Design and Performance Evaluation of a Portable Chamber for Prevention of Aerosol Airborne–Infection." *Journal of Advanced Research in Fluid Mechanics and Thermal Sciences* 100, no. 2 (2022): 181-197. https://doi.org/10.37934/arfmts.100.2.181197

[17] Fatma A-M. Kassem, Ahmed Farouk AbdelGawad, A. E. Abu El-Ezz a, Mofreh M. Nassief, and Mohamed Adel. "Investigation of Airflow Distributions in an Isolation Room to Reduce Airborne Infection." under review.

[18] Korkmaz, Gürsel, Mehmet Kılınç, Sevim Atmaca Razak, Münevver Ocak, Selma Korkmaz, and Y. Dilek Toprakkaya Kut. "Comparison of the performance properties of spunlaid non-woven fabrics used as face mask." *The Journal of The Textile Institute* (2022): 1-7. https://doi.org/10.1080/00405000.2022.2027073

[19] Sikdar, Partha, Gajanan S Bhat, Doug Hinchliffe, Shafiqul Islam, and Brian Condon. "Microstructure and physical properties of composite nonwovens produced by incorporating cotton fibers in elastic spunbond and meltblown webs for medical textiles." *Journal of Industrial Textiles* 51, no. 4_suppl (2022): 6028S-6050S. https://doi.org/10.1177/15280837211004287

[20] Yesil, Yalcin, and Gajanan S. Bhat. "Porosity and barrier properties of polyethylene meltblown nonwovens." *The Journal of the textile institute* 108, no. 6 (2017): 1035-1040. https://doi.org/10.1080/00405000.2016.1218109

[21] Thirumurugan, V., S. Karthikeyan, Kota Vinesh Kumar Reddy, and E. Murugan. "A Study on the Effects of Physical Properties and Thermal Properties of Nonwoven Fabric." *International Journal of Recent Advances in Multidisciplinary Topics* 2, no. 5 (2021): 8-10.

[22] Yan, Jing, Michael Grantham, Jovan Pantelic, P. Jacob Bueno de Mesquita, Barbara Albert, Fengjie Liu, Sheryl Ehrman, Donald K. Milton, and Emit Consortium. "Infectious virus in exhaled breath of symptomatic seasonal influenza cases from a college community." *Proceedings of the National Academy of Sciences* 115, no. 5 (2018): 1081-1086. https://doi.org/10.1073/pnas.1716561115

[23] Aliabadi, Amir A., Steven N. Rogak, Sheldon I. Green, and Karen H. Bartlett. "CFD simulation of human coughs and sneezes: a study in droplet dispersion, heat, and mass transfer." *In ASME International Mechanical Engineering Congress and Exposition*, vol. 44441, pp. 1051-1060. 2010. https://doi.org/10.1115/IMECE2010-37331

[24] Borro, Luca, Lorenzo Mazzei, Massimiliano Raponi, Prisco Piscitelli, Alessandro Miani, and Aurelio Secinaro. "The role of air conditioning in the diffusion of Sars-CoV-2 in indoor environments: a first computational fluid dynamic model, based on investigations performed at the Vatican State Children's hospital." *Environmental research* 193 (2021): 110343. https://doi.org/10.1016/j.envres.2020.110343

[25] King, M-F., Catherine J. Noakes, and P. Andrew Sleigh. "Modeling environmental contamination in hospital single- and four-bed rooms." *Indoor Air* 25, no. 6 (2015): 694-707. https://doi.org/10.1111/ina.12186

[26] Zayas, Gustavo, Ming C. Chiang, Eric Wong, Fred MacDonald, Carlos F. Lange, Ambikaipakan Senthilselvan, and Malcolm King. "Cough aerosol in healthy participants: fundamental knowledge to optimize droplet-spread infectious respiratory disease management." *BMC pulmonary medicine* 12, no. 1 (2012): 1-12. https://doi.org/10.1186/1471-2466-12-11

[27] Thatiparti, Deepthi Sharan, Urmila Ghia, and Kenneth R. Mead. "Computational fluid dynamics study on the influence of an alternate ventilation configuration on the possible flow path of infectious cough aerosols in a mock airborne infection isolation room." *Science and technology for the built environment* 23, no. 2 (2017): 355-366. https://doi.org/10.1080/23744731.2016.1222212

[28] Scharfman, B. E., A. H. Techet, J. W. M. Bush, and L. Bourouiba. "Visualization of sneeze ejecta: steps of fluid fragmentation leading to respiratory droplets." *Experiments in Fluids* 57, no. 2 (2016): 1-9. https://doi.org/10.1007/s00348-015-2078-4

[29] Portarapillo, Maria, and Almerinda Di Benedetto. "Methodology for risk assessment of COVID-19 pandemic propagation." *Journal of loss prevention in the process industries* 72 (2021): 104584. https://doi.org/10.1016/j.jlp.2021.104584

[30] Hui, D. S., M. T. Chan, and B. Chow. "Aerosol dispersion during various respiratory therapies: a risk assessment model of nosocomial infection to health care workers." Hong Kong Med J 20, no. Suppl 4 (2014): 9-13.

[31] Hui, David S. "Severe acute respiratory syndrome (SARS): lessons learnt in Hong Kong." *Journal of thoracic disease* 5, no. Suppl 2 (2013): S122. https://doi: 10.3978/j.issn.2072-1439.2013.06.18